Using three-dimensional CURVIC® contact models to predict stress concentration effects in an axisymmetric model

J. J. Rencis & S. R. Pisani
Department of Mechanical Engineering, University of Arkansas, USA

Abstract

CURVICs® are used to couple multiple rotors in an aircraft engine compressor, and are subjected to rotational loading. This work investigates three-dimensional boundary element contact models that contain the stage two aft and stage three forward CURVICs®. The three-dimensional models are used to estimate stress concentration effects in a finite element axisymmetric model under rotational loading. The three-dimensional models generated include a geometrically complex three-dimensional linear elastic body with curved surfaces that are analyzed with the BEASY® boundary element software package. The axisymmetric model uses the commercial finite element code ANSYS®.
Keywords: CURVIC, rotors, three-dimensional, axisymmetric, boundary element method, finite element method.

1 Introduction

CURVICs® are sometimes used in aircraft engine design where multiple rotor stacks are required. First introduced in 1942 by Gleason Works [1], a CURVIC® is a precision ground face spline. The CURVIC® allows torque transmission between individual rotors, and the self-centering feature of the CURVIC® face centralizes each rotor in the stack.

Stress analyses of CURVICs® at General Electric have incorporated both simple two-dimensional and more complex three-dimensional finite element analyses. Photoelastic and strain gage test results are used to substantiate the analyses, and extensive testing of individual components and rotor assemblies validate the CURVIC® life predictions. The more complex three-dimensional analyses and component testing are typically done after the design has been

established. Accurate and timely complex analyses are needed early in the design process.

In this work a simple axisymmetric finite element CURVIC® model using ANSYS® [3] is proposed for use in the early design stage. Since the axisymmetric model does not account for the true three-dimensional geometry of the CURVIC®, stress concentration factors are obtained from a three-dimensional boundary element model using BEASY® [2].

2 CURVIC®

CURVICs® are sometimes used in aircraft engine design to join rotating components so that they operate as a single unit. A typical CURVIC® application is the aircraft engine compressor shown in Fig. 1. This particular engine utilizes a five stage axial and one stage centrifugal compressor. The compressors job is to take ambient air from outside the engine and compress it. The compression is accomplished by a series of rotating blades and disks, which force the air through smaller and smaller areas. Once at a higher pressure (and temperature) the air will be mixed with fuel and combusted. The energy released during combustion is then converted to power the aircraft.

The rotating components that make up the compressor are shown in Fig. 2. The term CURVIC® refers to the teeth notched circumferentially in the front and back sides of the blisks. The blisks labelled in the figure are solid metal disks and blades machined from a single forging. The fact that the blades and disk are one continuous piece leads to the term 'blisk'. Each blisk in the assembly is stacked together and joined by the CURVICs® cut into the forward and aft faces of the blisks. This paper focuses on the stage 2 blisk aft and stage 3 forward CURVICs®. The stage 2 blisk aft is the life limiting location in the blisk.

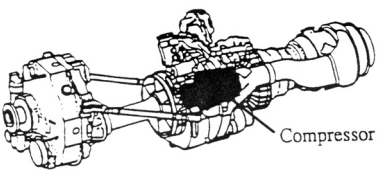

Figure 1: Aircraft engine with compressor area highlighted.

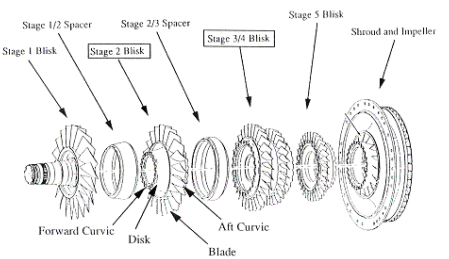

Figure 2: Compressor assembly.

3 Three-dimensional contact model

3.1 Geometry and material properties

Figure 3 shows the stage 2 and 3/4 blisks with the contact analysis regions highlighted. The contact models contain both the stage 2 aft and stage 3 forward CURVICs®. Figure 4 shows the axisymmetric finite element ANSYS® model (8-noded quadrilateral elements) that will be compared against the three-dimensional boundary element BEASY® model. An axisymmetric FEM model has been employed to analyze the compressor and to ensure that each component will be able to endure the loads it is subjected to during normal engine operation. Since the tierod (not shown) and parts of the blisks tend to be long and thin, i.e., has a large surface to volume ratio, FEM is better suited for axisymmetric analyses than BEM. The axisymmetric model supplies nominal stresses in the CURVICs®. The stresses are referred to as nominal because the geometric stress concentrations in the CURVIC® root (see Fig. 5) are not accounted for in the axisymmetric model. Since the CURVIC® is not an axisymmetric feature, three-dimensional modelling is required to predict the peak stress in the CURVICs® due to stress concentrations. The peak stress is then used to determine an appropriate theoretical stress concentration factor (k_t) which will be applied to the axisymmetric nominal stress results.

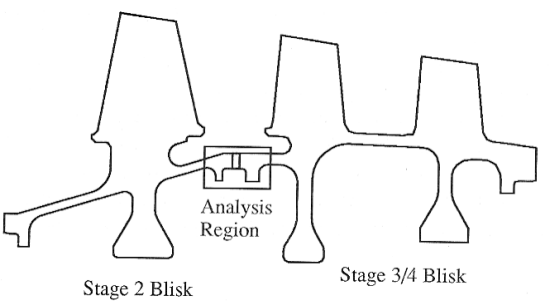

Figure 3: Stages 2 and 3/4 blisks showing contact model analysis region.

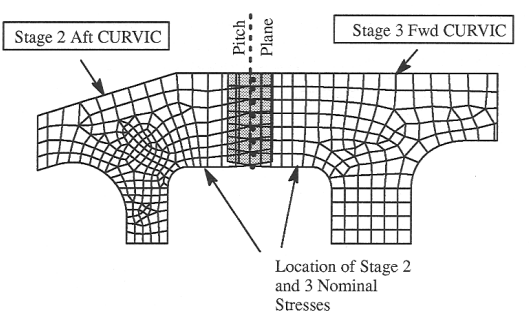

Figure 4: Axisymmetric finite element model to be compared to three-dimensional boundary element contact model.

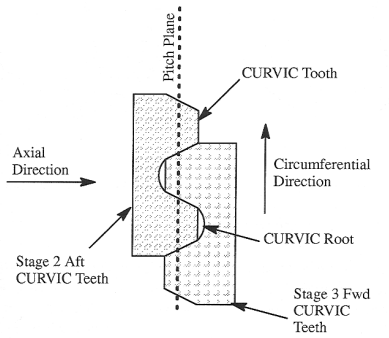

Figure 5: Radial view of mated CURVIC® pair.

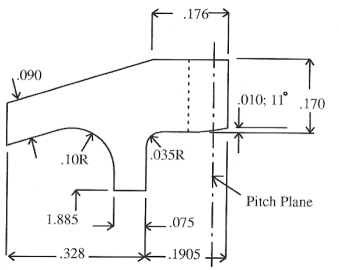

a. Arm geometry from a circumferential view.

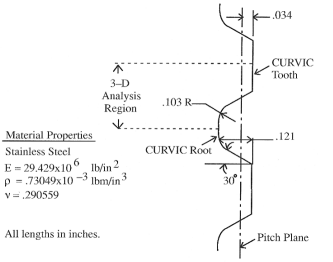

b. Geometry of teeth profile from a radial view.

Figure 6: Stage 2 aft CURVIC®.

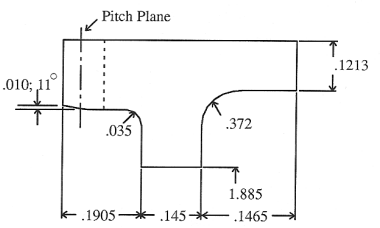

a. Arm geometry from a circumferential view.

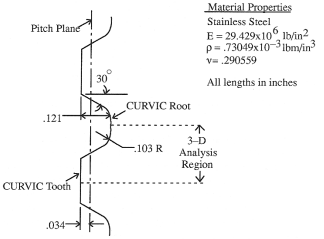

b. Geometry of teeth profile from a radial view.

Figure 7: Stage 3/4 forward CURVIC®.

The geometry for the stage 2 aft CURVIC® is shown in Fig. 6a and the CURVIC® teeth shown in Fig. 6b. The geometry for the blisk arm leading to the stage 3/4 forward CURVIC® is shown in Fig. 7a, with the profile of the CURVIC® teeth shown in Fig. 7b. The stage 3 forward CURVIC® teeth are identical to the stage 2 CURVIC® teeth, except that the tooth profile is concave. The mated components are symmetric for every 7.5° segment, therefore, the

three-dimensional BEM analysis is shown in Figs. 6b and 7b for the stage 2 and 3/4 blisks, respectively. Both the stage 2 and stage 3/4 blisks are made of stainless steel with the material properties shown in Figs. 6b and 7b.

3.2 Model generation and discretization

The contact model used surface patches to define a total of four zones in Fig. 8a. The main reason for creating the zones was to easily separate the two CURVICs® for pre- and post-processing, but a secondary reason was to reduce the overall solution time. Figure 8a shows the contact geometry and view of the separated zones. The location of the zones was chosen so that either the stage 2 aft CURVIC®, the stage 3 forward CURVIC® or the contact region could be isolated. The area of contact zone 1 is highlighted in Fig. 8a. Figure 8b shows the contact model mesh. Note that the mesh is relatively coarse, taking advantage of the BEM higher order mathematics and discontinuous elements. The mesh was generated using the BEASY® auto mesh generator, with 711 elements (BEASY® type Q2) and 3858 nodes created around the four zones. Each element has a quadratic geometry and linear displacement and traction surface functions.

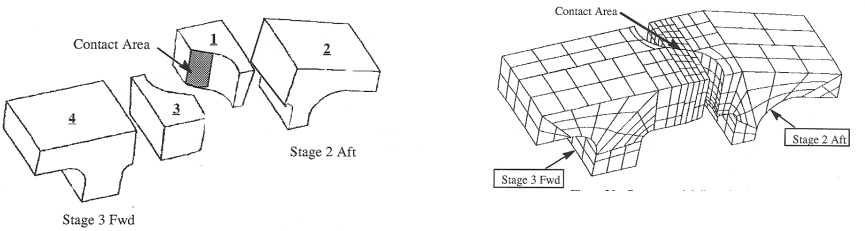

a. Geometry, zones and contact area. b. Discretization.

Figure 8: Three-dimensional contact model.

3.3 Loading cases and boundary conditions

The loads that are applied to the CURVIC® depend on how it is being used. Individual components may be tested to validate life prediction. The individual component is usually subjected to rotation only, cycling between a low and high speed to induce an alternating stress comparable to the stresses the part could see in actual engine operations. The cycling will usually continue until cracks appear in the critical areas. The number of cycles required to develop the crack are then compared with the analytical predications. In actual engine operations the CURVIC® loading will include the clamp load caused by the tierod and locknut, a clamp load wedge effect, and the body forces induced by rotation of the compressor. Thermal loads are also applied to the CURVICs® during engine operation, but their contribution is small because the CURVICs® are insulated from the compressor flowpath by the spacer rings (Fig. 2). Thermal effects were

considered negligible in this work. The contact model is subjected to three different load cases.

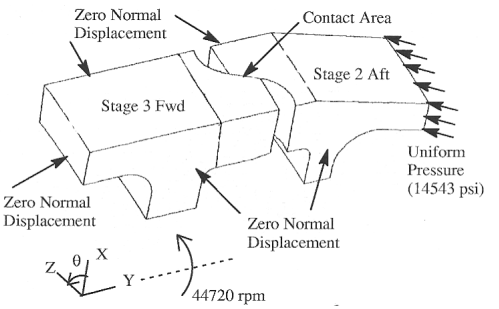

Figure 9: Contact model for general loading and boundary conditions. (Load cases 1, 2 and 3).

Load case 1 considered rotating the model about the Y-axis with a speed of 44720 rpm (4683.07 rad/sec) as shown in Fig. 9. The ends of both CURVICs® were restrained to zero Y-deflection to eliminate rigid body motion, and planes of symmetry (zero normal displacement) were defined at $\theta = 0^{\circ}$ (X-Y Plane) and $\theta = 7.5°$. The displacement constraints at the ends of the CURVICs® and Poisson's effect should cause the teeth to separate under the rotational loading.

Load case 2 loading and boundary conditions eliminated the rotation and added a clamp load. This condition reflects the state of the CURVIC when assembled in an engine and before the engine is started. The clamp load was applied as a uniform pressure (14543 psi) normal to the aft end of the stage 2 aft CURVIC®. The end of the stage 3 forward CURVIC® kept its zero axial displacement to eliminate rigid body motion along the axis of rotation.

Load case 3 loading and boundary conditions included both the clamp load and the rotation. This load case most closely represents the condition that the CURVICs will be subjected to in actual engine operation. The symmetry planes were still held to zero normal displacement, and the back of the stage 3 CURVIC® was forced to zero axial displacement. Figure 9 shows the contact model outline with all of the loading and boundary conditions indicated.

The surface between the stage 2 aft and stage 3 forward CURVICs® is specified to be a contact surface (Fig. 8a). A contact surface can be specified in BEASY® at any location where two zones meet. If the zone interface is assigned an initial gap (which may be positive, negative for an interference or zero), the BEASY® program will automatically assign a duplicate set of elements along the interface which are capable of simulating the contact. The version of BEASY® used in this work would not allow friction at the contact surface.

Each of the three load cases was applied to the axisymmetric finite element model of Fig. 4 to supply a nominal stress. The nominal stress is then used to determine a theoretical stress concentration factor (k_t) for the CURVIC® and is also be used to normalize the stresses in the stress contour plots. The non-linear

nature of the contact may cause the k_t for each loading condition to be different. However, it is desirable that the three-dimensional contact effects can be simulated in the axisymmetric model so that a single k_t can be used regardless of the applied loading.

4 Three-dimensional contact model stresses

4.1 Load case 1

The contact model for load case 1 considered only to rotational loading in Figure 9. The resulting Z-stress contours are shown for the entire model in Figures 10a and 10b, with close-ups of the stage 2 aft CURVIC® and stage 3 forward CURVIC® shown in Figures 11a and 11b, respectively. The results in Figures 10a, 10b and 10c are normalized to the nominal stress of the two-dimensional stage 2 aft CURVIC® (see Figure 4). The results shown in Figure 11b are normalized by the nominal stress of the axisymmetric stage 3 forward CURVIC® (Figure 4). Using the appropriate nominal stress allows a separate k_t to be determined for each CURVIC®. Note from Figures 10a, 10b and 10c that the resulting max k_t for the stage 2 aft CURVIC® is 1.84. A model of only the stage 2 aft CURVIC® was carried out and yielded a k_t of 1.89. This indicates that the contact condition had no impact on the final stresses. Similar results to the k_t models were expected based on the zero Y-displacement boundary conditions imposed on the front and back sides of the CURVICs®. The prescribed displacement conditions in Figure 9 allowed the CURVIC® teeth to separate under the applied loading. The result is in essence two separate k_t models, one for the stage 2 aft CURVIC® and one for the stage 3 forward CURVIC®.

The CURVIC® teeth separate because most of the hoop strain (93% of the total hoop strain) is concentrated in the CURVIC® root, not the CURVIC® teeth. The result is a larger space between the CURVIC® teeth on the blisk. In actual engine operation the clamp load will force the teeth on the neighbouring blisk to penetrate into the enlarged space, shortening the overall length of the compressor. For this model, however, the applied axial displacement prevented the teeth from clamping together. The effect is shown graphically in Fig. 12, where Δ_c is the change in space between the teeth and Δ_a is the amount of axial shortening in the CURVIC® joint.

Note from Fig. 11 that the k_t for the stage 3 forward CURVIC® is 1.89, which is identical to the k_t derived for the stage 2 aft CURVIC® in the more finely discretized models. These results indicate that each CURVIC® stage will have the same k_t regardless of whether the CURVIC® has a concave or a convex barrel shape as long as all the other geometric parameters are identical, i.e., fillet radius, tooth depth, etc.

4.2 Load case 2

Load case 2 is not presented due to space limitations of the paper.

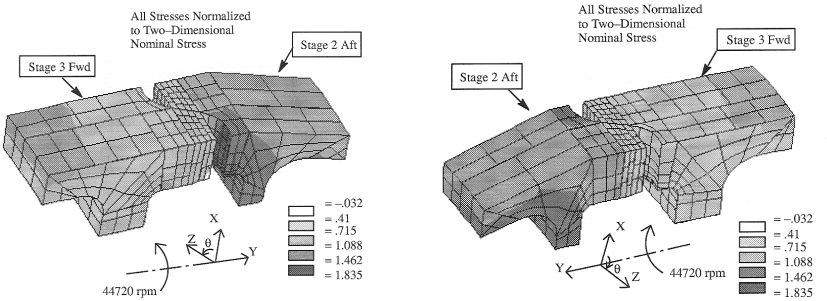

Figure 10: Load case 1 Z-stress results for assembly.

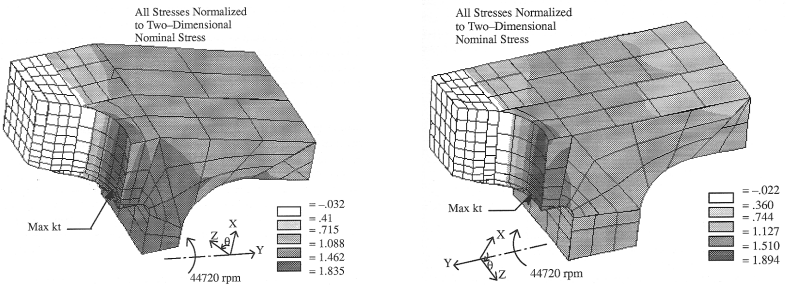

Figure 11: Load case 1 Z-stress results for stage 3 forward.

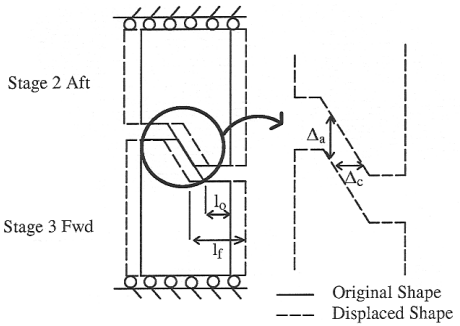

Figure 12: Radial view of CURVIC® teeth separation due to rotational loading, load case 1.

4.3 Load case 3

The results for load case 3 are shown in Figs. 13a and 13b for views 1 and 2, respectively, again show a peak stress occurs in the stage 2 aft CURVIC. The results also prove that this load case is the most severe, with the maximum stress

in the stage 2 aft CURVIC nearly twice as high as in load case 1 and nearly three times greater than load case 2 (not shown).

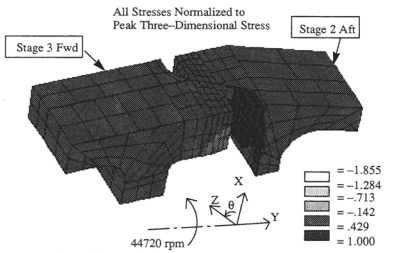

Figure 60: BEASY load set 3 Z–stress results, view 1.

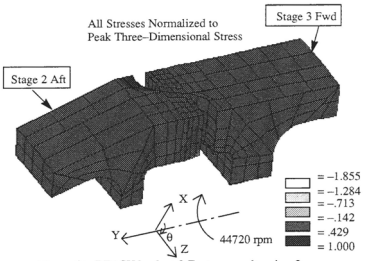

Figure 61: BEASY load set 3 Z–stress results, view 2.

a. View 1. b. View 2.

Figure 13: Load case 3 Z-stress results.

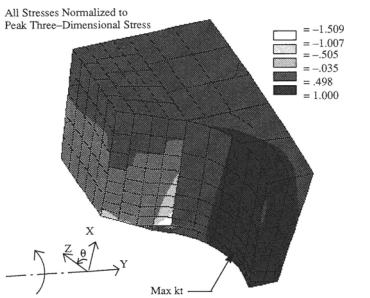

Figure 62: BEASY load set 3 stage 2 aft CURVIC root Z–stress results, view 1

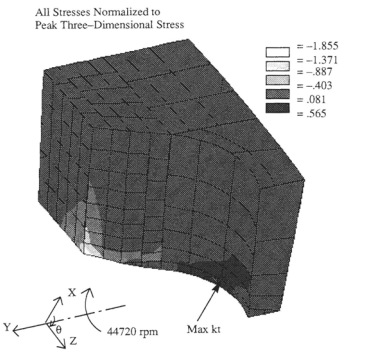

Figure 63: BEASY load set 3 Stage 3 Fwd CURVIC root Z–stress results, view 2.

a. View 1. b. View 2.

Figure 14: Load case 3 stage 2 aft CURVIC root Z-stress results.

A grey scale plot of the stage 2 aft CURVIC stress contours are shown in Fig. 14a. The stage 3 forward CURVIC shown in Fig. 14b still has its peak stress occur in the CURVIC root, but the magnitude of the stress is only 56% of the stage 2 aft CURVIC. The results from load case 3 also verify the non-linearity of CURVIC behaviour. If this contact analysis were linear the results from loads cases 1 and 2 could be added to obtain load case 3. However, the contact condition between the CURVICs is non-linear and can change with loading. The contact in load case 2 is different from the contact in load case 3 because the rotational loading in load case 3 changes the orientation of the CURVIC teeth. The end result is that the sum of the maximum stresses from load cases 1 and 2 is 12% lower than the maximum stress in load case 3.

5 Applying contact model results to axisymmetric models

One goal of this work is to duplicate the stress state of a three-dimensional model in an axisymmetric model. For example, using a rotational loading in load case 1 and a k_t in an axisymmetric model to yield the same peak stress as the three-dimensional contact models. It has been pointed out that the k_t for the CURVICs® under rotational loading is approximately 1.89. The 1.89 rotational k_t can be used to predict the stresses for a single component (non-contacting) at any rotational speed.

6 Conclusion

A simple axisymmetric finite element model has been proposed for carrying out a stress analysis in the early design stage. When subjected to rotational loading only, the k_t for a convex and concave CURVIC® are the same (provided that all other major geometric and material characteristics are identical). This result eliminates the need to create separate k_t models for CURVICs® that differ only in their barrel shape, and may allow different components with similar CURVICs® to be tested without creating new three-dimensional models for every load case.

7 Future work

Intuitively, the non-linear nature of the contact between the CURVICs® implies that a single k_t cannot be established to represent more than one load case. However, the CURVICs® are always subjected to clamp loading and contact in actual engine operation (the CURVISs® never separate), which may eliminate or make the non-linear nature of contact very small. If the wedge effects can then be translated into an equivalent radial force it may be possible to develop a single k_t for the contacting CURVICs®. The application of the wedge effect force was tested through three axisymmetric models. The first model was subjected to a clamp load, but no wedge effect force was applied. The second model was subjected to a clamp load and included the wedge effect force. The third model included the clamp load, wedge effect force and rotational loading. These cases will be discussed in a future paper.

References

[1] CURVIC is a registered trademark of The Gleason Works, 1000 University Avenue, Rochester, NY, 14603, USA.
[2] BEASY is a registered trademark of Computational Mechanics, U.K. BEASY Ltd., Ashurst Lodge, Southampton, SO4 2AA, http://www.beasy.com/.
[3] ANSYS is a registered trademark of ANSYS Inc., 275 Technology Drive, Canonsburg, PA, 15317, USA, http://www.ansys.com/.